ERJ
Engineering Research Journal
Faculty of Engineering
Minoufiya University

# Vector Control of FSTP Inverter Fed Synchronous Reluctance Motor Based Maximum Torque Control

**Haitham. Z. Azazi**
*Department of electrical Engineering*
*Menoufiya University*
*Menoufiya, Egypt*
.haitham_azazi@yahoo.com

**M. K. Metwally**
*Department of electrical Engineering*
*Menoufiya University*
*Menoufiya, Egypt*
*mohkamel2007@yahoo.com*

**Abstrac:**
This paper presents a cost-effective vector control strategy for four switch three phase (FSTP) inverter fed a synchronous reluctance motor with conventional rotor (SynRM) drive. The reduction of the number of power switches from six to four improves the cost-effectiveness, volume-compactness and reliability of the three phase inverters. In this paper, a simulation model of the drive system is developed and analyzed in order to verify the effectiveness of the proposed approach. The application of vector control to a SynRM at maximum torque control (MTC) operation is presented with emphasis on the effects of saturation and iron losses are briefly considered. A PI controller is used to process the speed error. Two independent hysteresis current controllers with a suitable hysteresis band are utilized for inverter switches signals. A simplified steady-state d-q model including saturation and iron losses is presented. Simulation and experimental results show that the drive system provides a fast speed response and good disturbance rejection capability.

يقدم هذا البحث تقنية التحكم الاتجاهي باستخدام طريقة فعالة من حيث التكلفة بواسطة عاكس كهربي بأربعة مفاتيح لتسيير محرك تزامني ذو الممانعة بعضو دوار تقليدي. بتقليل عدد مفاتيح القدرة من ستة إلي أربعة يحسن التكلفة والحجم والأعتمادية للعواكس الكهربية ثلاثية الأوجه. تم تحليل وعرض النموذج المحاكي لمنظومة التسيير وذلك لتوضيح كفاءة الطريقة المقترحة. تم تطبيق التحكم الأتجاهي علي المحرك التزامني ذو الممانعة عند التشغيل والتحكم بأقصي عزم مع الأخذ في الأعتبار تأثير التشبع والمفاقيد الحديدية . تم استخدامه الحاكم التكاملي التناسبي لإجراء التحكم في السرعة. تم استخدامهما اثنين من حواكم التيار ذو التخلفية منفصلين بمدي تخلفية مناسب لتغذية الإشارات لمفاتيح العاكس الكهربي. تم عرض النموذج المبسط للآلة في حالة الأستقرار مع الأخذ في الأعتبار تأثير التشبع والمفاقيد الحديدية. أثبتت النتائج النظرية والعملية أن منظومة التسيير تعطي أستجابة سريعة للسرعة ومقدرة عالية علي تحمل الأضطرابات.

***Keywords***: *Conventional Synchronous Reluctance motor; Four switch inverter; Vector control, Maximum torque control; Hysteresis current controller; Saturation and iron losses.*

## I. INTRODUCTION

Inverter driven synchronous reluctance motors are a good choice for many variable-speed drive systems. Today's variable-speed industrial drives are mostly based on standard two or four-pole induction motors. These applications are also suitable for synchronous reluctance motors. The first rotating magnetic-field synchronous motor was, however, introduced by Kostko in 1923 [1]. Traditionally, synchronous reluctance motors are used directly online with a rotor cage, because pure synchronous reluctance motors do not have a starting torque characteristic [2], [3]. Nowadays, by using modern inverter technology, suitable field-oriented control and a pulse width modulation (PWM) technique, the machine without the rotor cage can still be started.

The advantages of the synchronous reluctance motors with variable-speed drive are mentioned in [4]. They are of simple rotor construction with no vital need for the rotor cage in speed controlled drives, have no rotor resistive losses, with low-inertia, synchronous running and easy speed control without encoders. They also have easy field weakening compared to synchronous permanent-magnet motors. Although, synchronous permanent-magnet motors are also a good choice for many variable-speed drive applications, the advantages of using synchronous reluctance motors, as opposed to permanent-magnet motors, is that expensive magnets are not needed. It is also introduced permanent magnets-assisted synchronous reluctance machines where properties of synchronous reluctance and permanent magnet machines are combined [5]. An additional benefit of synchronous reluctance motors is material saving. They could be produced with similar kinds of methods as synchronous permanent-magnet motors and induction motors. However, there

are many difficulties in producing them, such as complex structures and costly machining.

The invention of high speed power semiconductor device makes it possible to control the AC drives with six switch three phase (SSTP) inverters. This inverter was popular since the last few decades. But these inverters have some disadvantages such as losses in the six switches, complexity of the control algorithms and generating six pulse width modulated (PWM) logic signals [6-9]. In recent years, many researches and development projects focusing on the cost reduction of SynRM drive had been developed. In [6] an AC to AC converter with least amount of hardware was proposed for three phase induction motor (IM) drive. A cost effective four switch three phase (FSTP) inverter was proposed for IM drive in [7]. The authors showed a performance comparison of the FSTP inverter fed drive with SSTP inverter fed drive in terms of speed response and total harmonic distortion of the stator current. The authors also proposed fuzzy logic based control scheme for FSTP fed interior permanent magnet (IPM) synchronous motor drive [8]. A vector control technique for IM using FSTP inverter was presented for high performance industrial drive systems in [9]. Issues such as efficiency and torque/ampere are important in evaluating the performance of an electric machine. Such characteristics depend on the losses and saturation behavior of the machine. However, a model is very useful in understanding the way in which various losses and nonlinearities impact performance. To assist in this regard, a synchronous reference frame steady state model of a SynRM including saturation and iron losses is presented [10]. The behavior of a vector-controlled SynRM is analyzed based on this model.

In this paper, the close loop vector control scheme at maximum control operation of the SynRM drive fed by FSTP inverter with a simple PI controller has been simulated in MATLAB/SIMULINK environment. The hysteresis controller is used to control the motor current so that it can follow the command current as close as possible to the sinusoidal reference.

A comparison of FSTP inverter fed SynRM drive performance with and without including the effects of saturation and iron loss is also made in terms of speed response, torque response, and stator current response under identical operating conditions.

## II. Equivalent Circuit of Synchronous Reluctance Motor and Mathematical Model

The mathematical model of the SynRM is required for accurate representation of the system. Fig. 1 (a), shows the equivalent circuit of a synchronous reluctance machine equipped with three phase, symmetrical, sinusoidally distributed windings. Conceptually, a resistor $R_m$ coupled to the total stator flux is added to incorporate iron losses. This resistor can be used to account for the main flux core losses in the stator iron. The resulting steady-state *d-q* equivalent circuits are shown in Fig. 1(b). The dynamic model which describes the behavior of the conventional rotor SynRM in the synchronously rotating d-q reference frame without iron loss effect can be expressed as follows [11]:

$$v_d = R_s i_{ds} + L_d \frac{di_{ds}}{dt} - \omega_r L_q i_{qs} \quad (1)$$

$$v_q = R_s i_{qs} + L_q \frac{di_{qs}}{dt} + \omega_r L_d i_{ds} \quad (2)$$

where the $v_d$ and $v_q$ are *d*- and *q*- axis terminal stator voltages, respectively. The $i_{ds}$ and $i_{qs}$ are, respectively, *d*- axis and *q*- axis torque producing currents. The $L_d$ and $L_q$ are the *d*- and *q*- axis self inductances, respectively. The $R_s$ is the stator resistance and $\omega_r$ is the rotor speed. The developed electromagnetic torque is given as:

$$T_e = \frac{3P_p}{2}(L_d - L_q) i_{ds} i_{qs} \quad (3)$$

The mechanical motion of the SynRM can be expressed as:

$$T_e = T_L + J_m \frac{d\omega_r}{dt} + B_m \omega_r \quad (4)$$

where $P_p$, $T_L$, $J_m$, and $B_m$ are the number of pole pairs, the load torque, the moment of inertia of rotor and the viscous friction coefficient, respectively.

The treatment of saturation has been considered in detail by a number of authors [12]-[13], and numerous methods with varying levels of complexity are available. In this paper, the first-order approximation of simply representing the relation between $\lambda_{ds}$ and $i_{dm}$, by a saturation curve is employed. It is assumed, and confirmed by the results, that the *q* axis does not saturate significantly and that there is negligible cross coupling between the *d* and *q* axis caused by saturation.

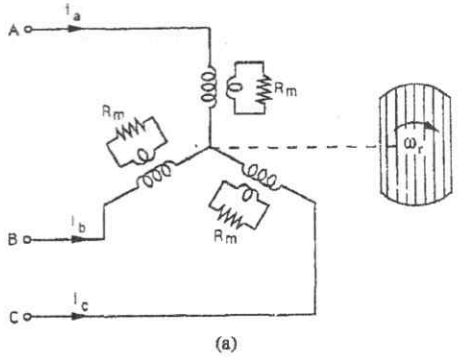

(a)

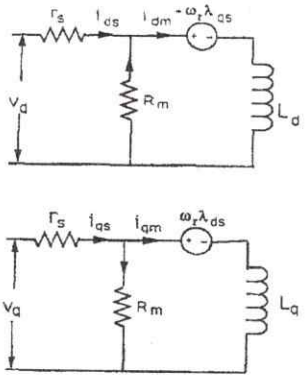


(b)

**Fig. 1**: Structure and equivalent circuit of a SynRM: (a) Structure of a SynRM; (b) equivalent circuit in rotor reference frame.

Note the difference between the current pair ($i_{qm}$, $i_{dm}$) compared with ($i_{qs}$, $i_{ds}$). If the iron loss is neglected, i.e., $R_m$ approaches infinity, these two current pairs become equal. In this case, the stator MMF is aligned with the stator current. When $R_m$ is finite, however, a phase difference between the stator current and MMF occurs due to the current in $R_m$. The relation between vectors $I_{dqs}$ , $I_{dqm}$ and $\lambda_{dqs}$ is shown in Fig. 2. The electromagnetic torque produced can be obtained based on the energy balance and the induced speed voltage as.

$$T_e = \frac{3}{2}(\lambda_{ds} i_{qm} - \lambda_{qs} i_{dm}) \quad (5)$$

The torque is interpreted as the interaction between the flux linkage $\lambda_{dqs}$ and the current $i_{dqm}$ and it is assumed that the effect of the flux non-linearity can be taken into account by means of the saturation curve relating $\lambda_{ds}$ and the current $i_{dm}$. The torque equation and the circuits of Fig. 1 (b) form a useful conceptual and first-order analytical model to assist in understanding saturation and core loss impacts on SynRM performance.

## III. Vector Control of a SynRM Without Saturation and Iron Losses

When saturation and iron losses are neglected, $R_m$ approaches infinity. The $d$-$q$ quantities are decoupled in this case. It is often desirable to achieve optimal efficiency operation of a SynRM. This can be achieved by selecting an appropriate current angle $\theta$ with respect to the rotor $d$ axis as shown in Fig. 2. It can be easily shown that the optimal angle is 45° for maximum torque control "MTC" [13], without saturation and iron losses.

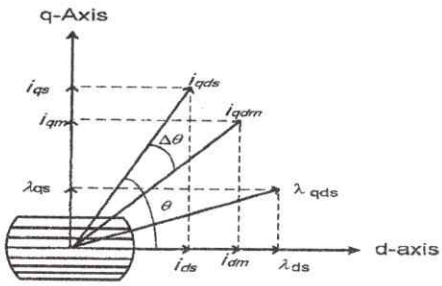


**Fig. 2** Vector diagram of a SynRM for finite $R_m$

## IV. Effects on Vector Control Caused by Saturation and Iron Loss

An approach to include the saturation effect of the iron is to assume that the torque equation remains true except that inductances in the $d$ and $q$ axis are excitation-current dependant. Note in particular that the saturation effect in the $d$ axis is expected to be very different from that of the $q$ axis because the nature of the magnetic paths is different. In the $d$ axis, the magnetic path is iron dominant and excitation sensitive, whereas in the $q$ axis, the magnetic path is air dominant and not excitation sensitive. Hence, an unequal saturation effect occurs on the $d$ and the $q$ axis, respectively, as the current increases.

Under such a circumstance, to properly control the angle $\theta$ to optimally allocate the components $i_{ds}$, $i_{qs}$ becomes complicated. While saturation alone increases the complexity of vector control, the iron loss will further complicate the situation. As illustrated by the $d$-$q$ transformation, to represent the effect of the iron loss, an additional resistor $R_m$ needs to be added to the equivalent circuit. It is of importance to realize that in the vector-controlled synchronous reluctance motor, the shunting resistor will share the input stator current. Hence, the physical stator currents are no longer the currents that directly govern the electromagnetic torque.

In effect, a new magnetizing current $I_{qdm}$ is defined by the component currents $I_{qm}$ and $I_{dm}$ as is shown in Fig. 2. Comparing vectors $I_{qds}$ and $I_{qdm}$ shows that an additional angle shift $\Delta\theta$ is generated due to the iron loss. In effect, $R_m$ adds an additional coupling mechanism to the $d$ and $q$ circuits, which can aggravate the misplaced stator current vector. It is evident that controling the current components $i_{dm}$ $i_{qm}$ via vector control of the stator MMF for optimal MTC or optimal efficiency operation becomes more complicated.

## V. FSTP Inverter Model

Fig. 3 shows the power circuit of the four switch inverter fed SynRM drive. A three phase system is obtained by connecting the phase 'c' terminal of the stator windings directly to the centre tap of the DC

link capacitors. The single phase AC supply is used to level the output DC voltage.If $V_{dc}$ is the maximum voltage across the DC link capacitors, and $S_a$, $S_b$ are the states of power switches for each phase, then three phase voltages of the SynRM can be expressed as follows [8]:

$$V_a = \frac{V_{dc}}{3}[4S_a - 2S_b - 1] \quad (6)$$

$$V_b = \frac{V_{dc}}{3}[4S_b - 2S_a - 1] \quad (7)$$

$$V_c = \frac{2V_{dc}}{3}[-S_a - S_b + 1] \quad (8)$$

If $S_a = 1$ then $T_1$ is on and $T_2$ is off; If $S_a = 0$ then $T_1$ is off
and $T_2$ is on.
If $S_b = 1$ then $T_3$ is on and $T_4$ is off; If $S_b = 0$ then $T_3$ is off and $T_2$ is on.

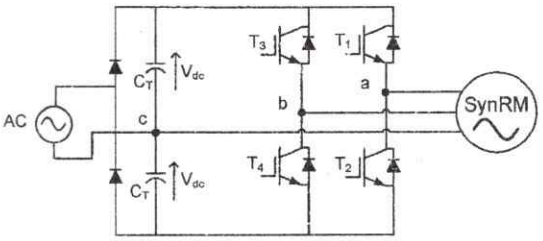


**Fig. 3**: Power circuit of the drive system.

## VI. CONTROL SCHEME

The vector control scheme is shown in Fig. 4. The speed error is processed through a PI controller to generate the torque producing component of the stator current ($i_q^*$). The magnetizing component of the stator currents $i_d^*$ along with $i_q^*$ are then used to generate the reference currents $i_a^*$, $i_b^*$, and $i_c^*$. Two independent hysteresis current controller with a suitable hysteresis band are used to command the motor currents $i_a$, and $i_b$ to follow the reference currents. The hysteresis controllers also generate four switching signals which will fire the power semiconductor devices of the three phase inverter to produce the actual voltages to the motor with and without saturation and iron loss effect at MTC operation.

rectified by the front-end rectifier. The capacitors are

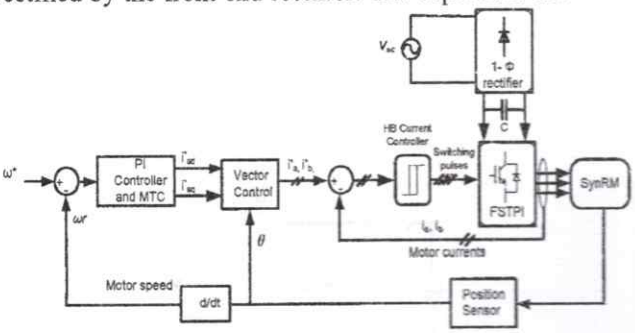


**Fig. 4**: Block Diagram of Vector Control Scheme

## VI. SIMULATION RESULTS

The proposed methodology above is simulated using SIMULINK/MATLAB software, where a simulation model of the drive system and the motor model including saturation and iron losses is developed and analyzed in order to verify the proposed approach effectiveness. A PI controller is employed to track the rotor speed and fix it at constant specified value. Two independent hysteresis current controllers with a suitable hysteresis band are utilized for inverter switching. Two cases have been studied, saturated and unsaturated inductances conventional rotor SynRM. A three phase SynRM machine of rating 0.75 kW with conventional rotor type is used in this drive system. The parameters of which are reported in table 1. The incremental time $\Delta t$ for simulating the system is 50μs.

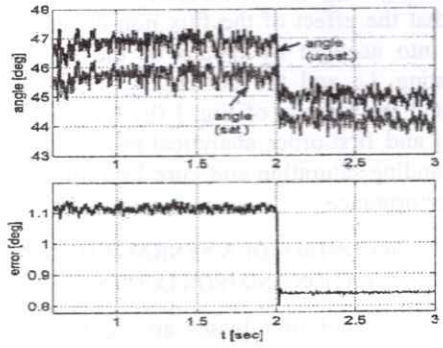


(a)

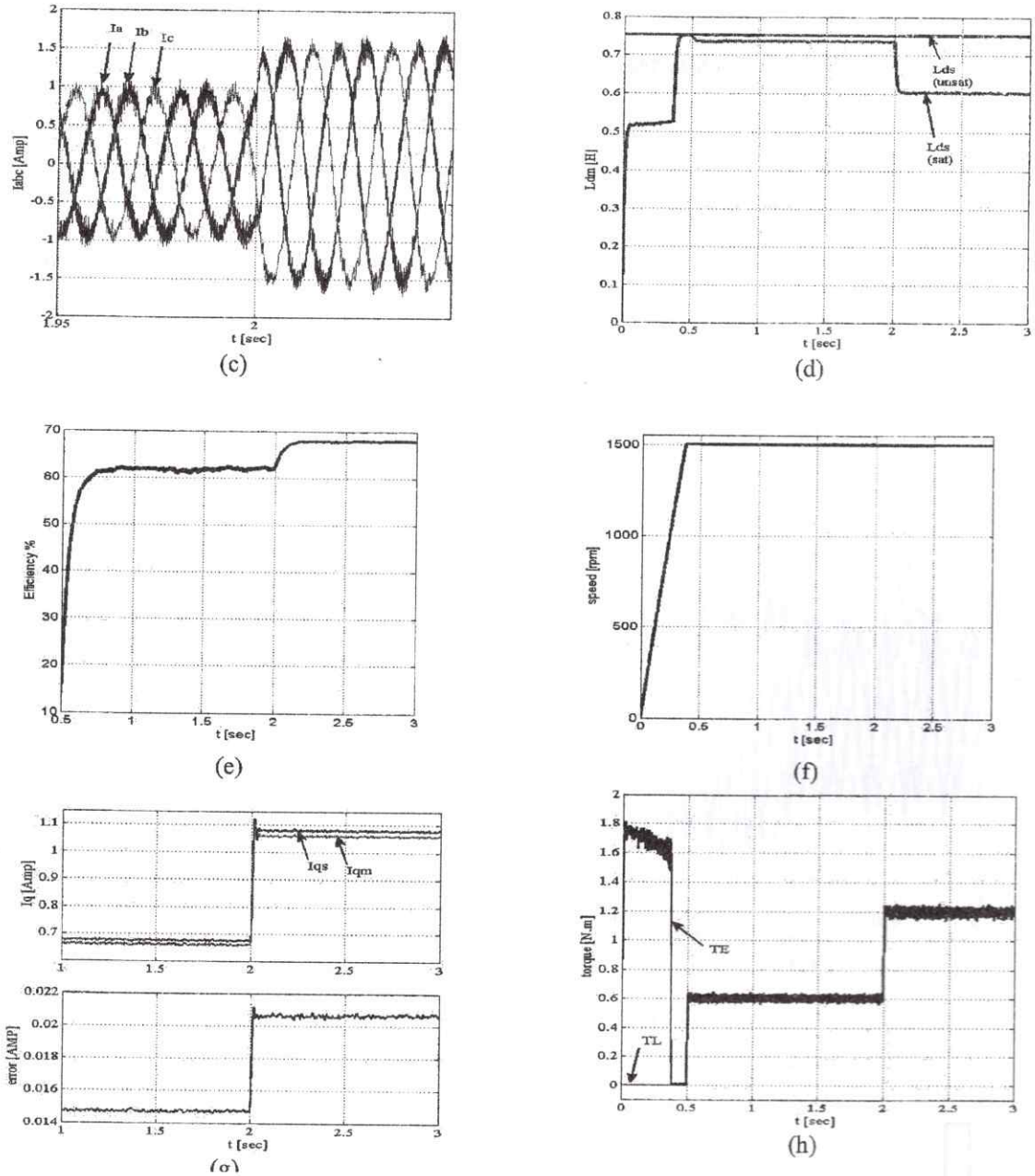


Figure 5. The conventional rotor SynRM performance with load change from no load to half to full loads at 0.5s and 2s, (a) angles considering saturation and neglecting saturation at maximum torque control and the difference between them, (b) the saturated direct axis stator current (Idm) and the unsaturated direct axis stator current (Ids) and the error between them , (c) the abc motor currents, (d) the d-axis saturated and unsaturated inductances, (e) the CSynRM efficiency, (f) the rotor speed, (g) the saturated q- axis stator current (Iqm) and the unsaturated q- axis stator current (Iqs) and the error between them , (h) the motor torque.

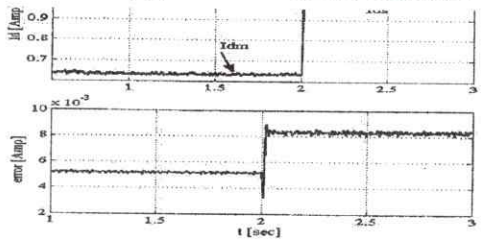


(b)

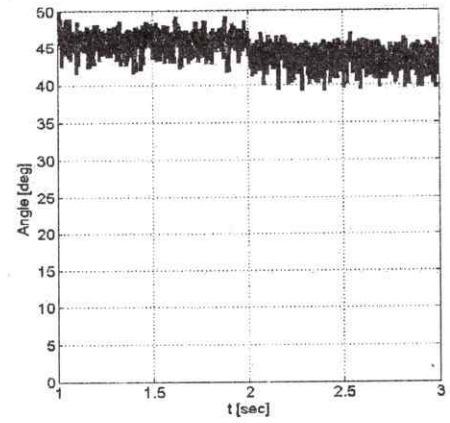


(a)

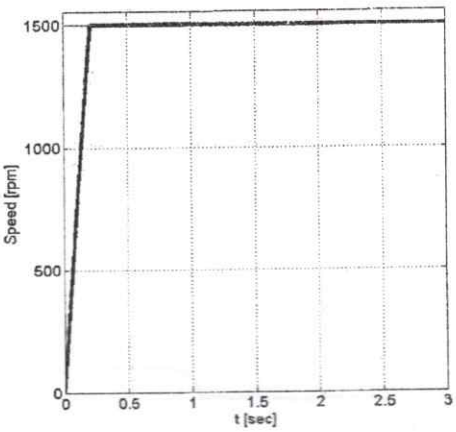


(b)

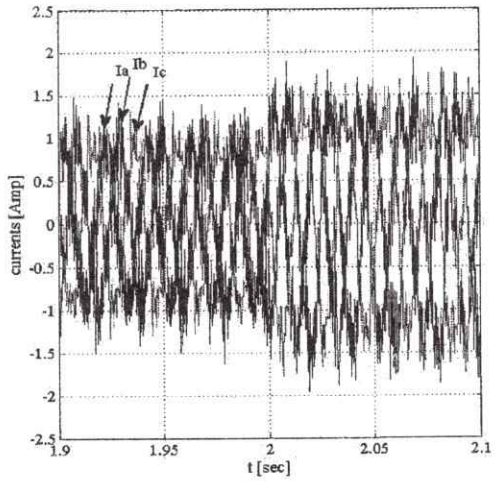


(c)

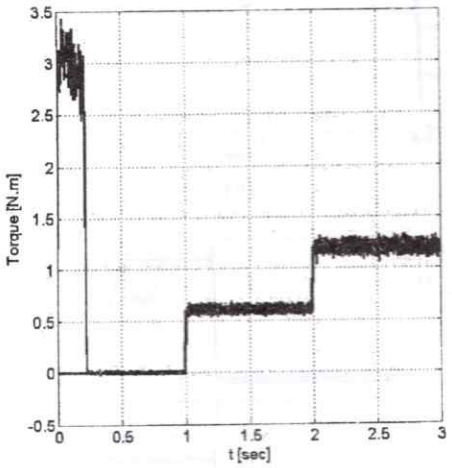


(d)

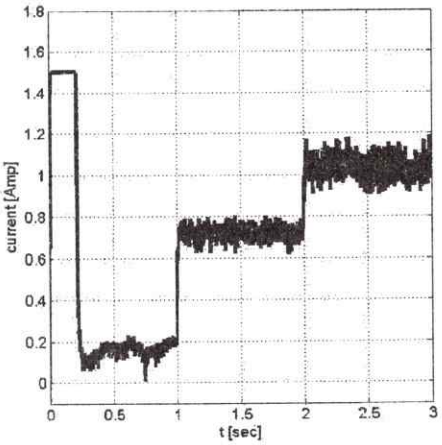


(e)

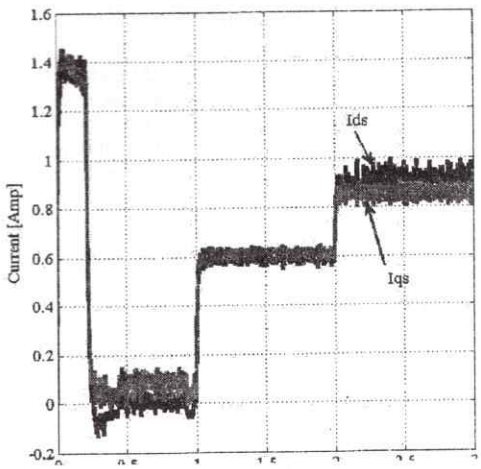


Figure 6. The conventional rotor SynRM unsaturated performance with load change from no load to half to full loads at 1s and 2s, (a) the angle of MTC, (b) the rotor speed, (c) the abc motor currents, (d) the motor torque, (e) the reference d-q axis currents, (f) the motor d-q axis currents.

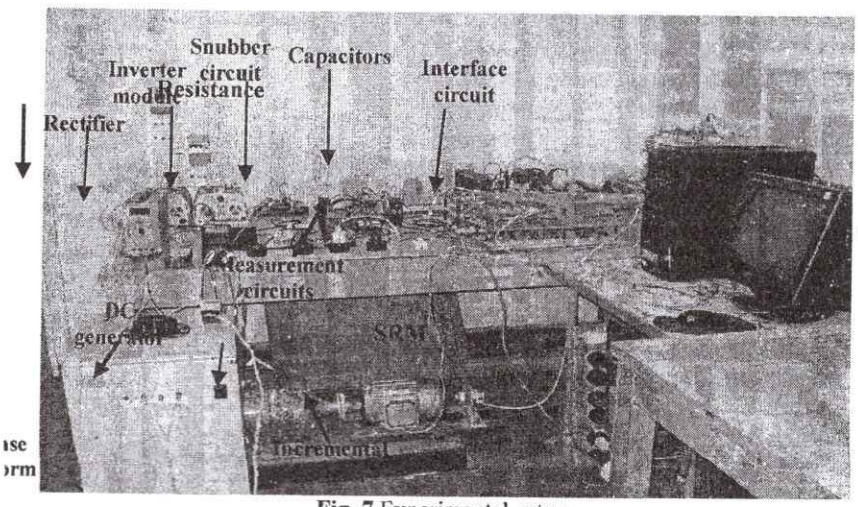


**Fig. 7** Experimental-setup

TABLE 1: SYNRM WITH CONVENTIONAL ROTOR PARAMETERS

| | |
|---|---|
| Number of pole pair: $P_P$ | 2 |
| Stator resistance: $R_s$ | 14 Ω |
| Iron loss Resistance: $R_m$ | 1000 Ω |
| *d*-axis inductance: $L_d$ | 0.4552 H |
| *q*-axis inductance: $L_q$ | 0.1432H |
| Motor inertia: $J_m$ | 0.001 Kg-m$^2$ |
| Friction coefficient: $B_m$ | 0.0001 N-m/rad/sec |

Figs. 5, 6 show the performances of the conventional rotor SynRM with saturated and unsaturated inductances, respectively. In Fig. 5, the conventional rotor SynRM performance is simulated with load change from no load to half load to full loads at 0.5s and 2s, respectively, while Fig. 6 shows the conventional rotor SynRM performances with load change from no load to half load to full load at 1s and 2s, respectively. Fig. 5(a) gives the saturated and unsaturated angles at MTC which is approximately equal 45 degree. The unsaturated angle is greater that the saturated with about 1 degree as shown in Fig. 5(a) lower figure.

Fig. 5(b) shows the saturated direct axis stator current $I_{dm}$ ($I_{dm}$) and the unsaturated direct axis stator current ($I_{ds}$) and the error between them. The simulation shows $I_{dm}$ is greater than $I_{ds}$ with about 5mA or 9 mA when the load changes from half to full loads. Fig. 5(c) gives the three phase sinusoidal motor currents and they form a balanced three phase system. The employed controller can recover the balanced system fast after the load change. Fig. 5(d) shows the direct axis saturated ($L_{dm}$) and unsaturated ($L_d$) inductances. The unsaturated inductance is 0.75H and the saturated decreased from about 0.72H to about 0.6H when the load changes from half to full load. The efficiency increases from about 60% to about 68% when the load increases from half to full load as shown in Fig. 5(e). The motor speed builds up to the rated value 1500 rpm in about 0.4s as shown in Fig. 5(f). The saturated q- axis stator current ($I_{qm}$) and the unsaturated q- axis stator current ($I_{qs}$) and the error between them are shown in Fig. 5(g), where $I_{qs}$ is greater than $I_{qm}$ with about 0.02A.

The motor torque is shown in Fig. 5(h), it changes from 0.6Nm to 1.2 Nm for half load and full load, respectively.

Fig. (6) shows the CSynRM performances for unsaturated inductance. The angle of the MTC is achieved and it is found to be approximately 45°. The motor speed builds up to its rated value 1500 rpm within 0.3s as shown in Fig. 6(b). Fig. 6(c) gives the three phase sinusoidal motor currents which form a balanced three phase system. it can be noted that the employed controller can recover the balanced system fast after the load step change. The operation of the motor is tested at no load, half load and full load and the torque is simulated in Fig. 6(d) and found to be 0.6 Nm and 1.2 Nm for half load and full load respectively. Fig. 6(e) and (f) illustrate the reference d-q axis currents and the motor d-q axis currents.

## V. EXPERIMENTAL RESULTS

The experimental setup is carried out by a DSpace 1104 system with I/O card for real time control (sampling time: Ts= 5e-5). An interface board was build to receive the gate-drive signal, isolated them and connected to the four switches which were implemented using integrated IGBT 100A. The output from FSTPI was connected to a three phase induction motor. The experimental results shown are

from the conventional rotor SynRM drive coupled to a separately excited DC generator working as a load as shown in Fig .7 The machine under test was operated under maximum torque control operation. The torque is applied by the DC generator under torque controlled mode. An optional position signal is available from an encoder with 1024 pulses per revolution.

Figure 8 shows the motor performance with load change from no load to full load and then back to no load at 3s and 7s respectively at constant speed equal to 1500 rpm. Fig.8a shows the speed, torque, and saturated inductance of the motor. Fig. 8b shows the d-q axis motor current and Fig. 8c shows the motor Iabc current when load change from zero to full load torque. The results show the effectiveness of the proposed method during transient response.

Also Fig. 9 shows the motor performance when speed change from 0 rpm to 900 rpm and to 1500 rpm at 1s and 5s respectively at full load torque.

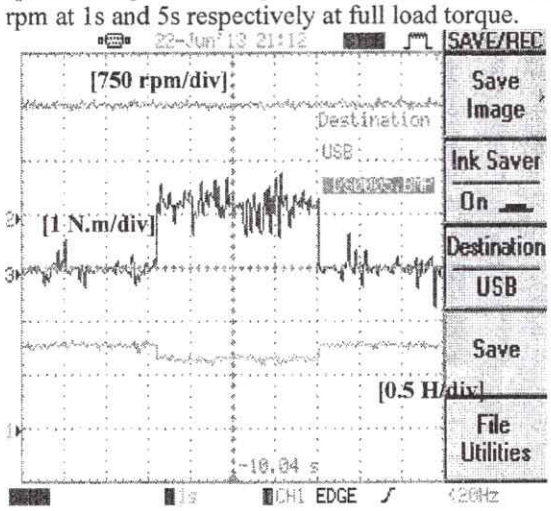


(a) Upper the rotor speed, middle the motor torque, and lower the saturated inductance Ldm.

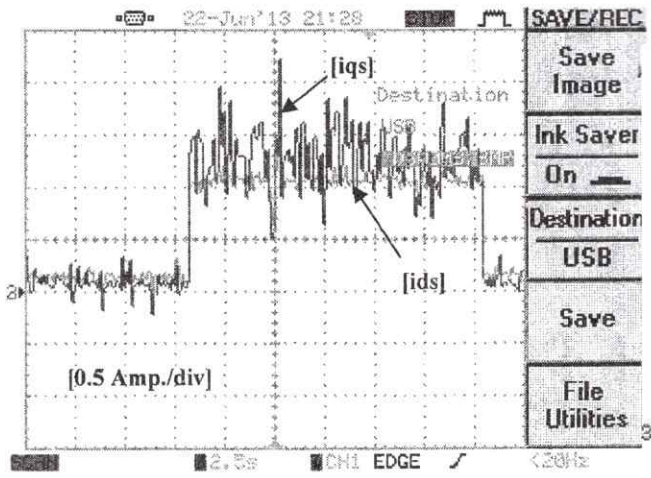


(b) The motor d-q axis currents.

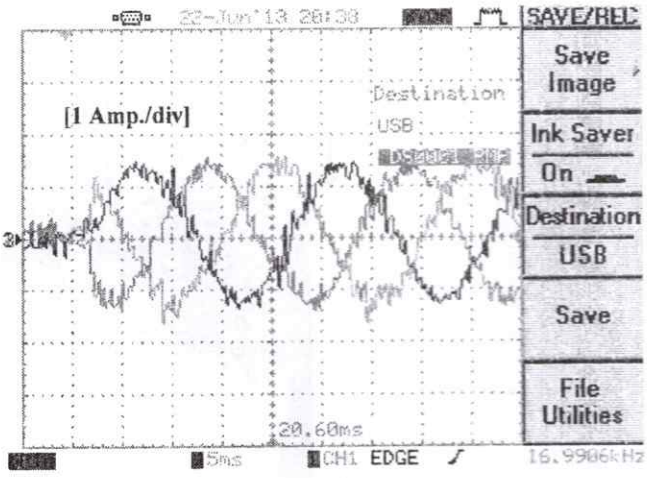


(c) The motor Iabc stator currents.

Figure. 8: The conventional rotor SynRM saturated performance with load change from no load to full load to no loads at 3s and 7s with speed = 1500 rpm.

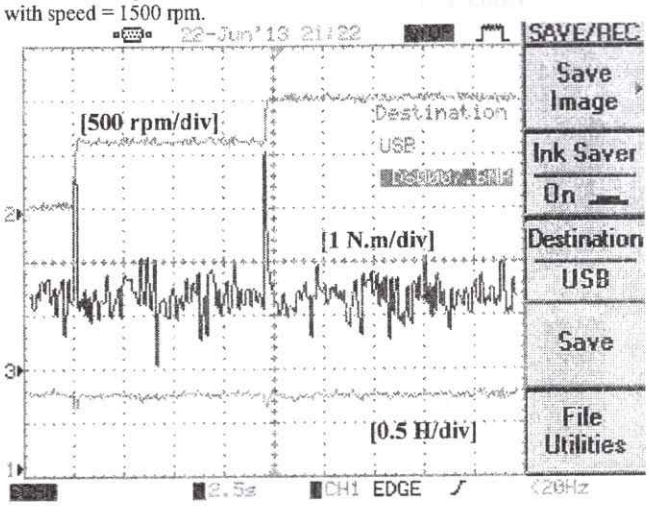


(a) Upper the rotor speed, middle the motor torque, and lower the saturated inductance Ldm.

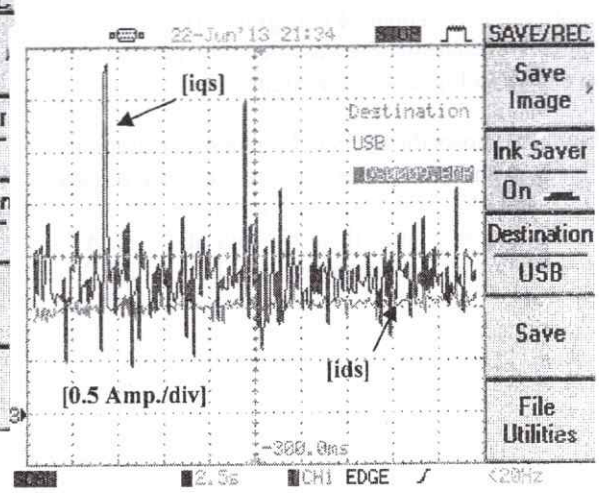


(b) The motor d-q axis currents.

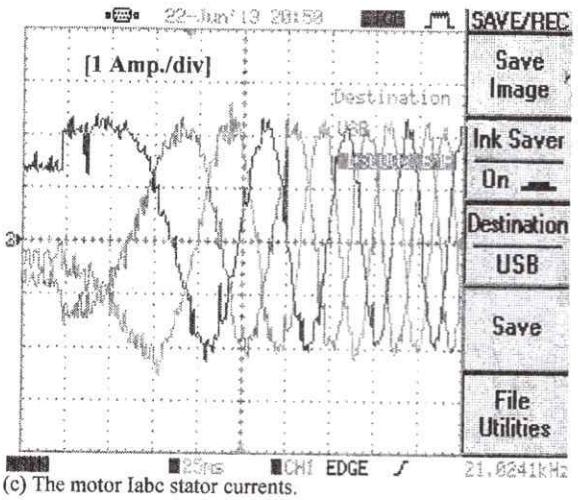


(c) The motor Iabc stator currents.

Figure. 9: The conventional rotor SynRM saturated performance with speed change from 0 rpm to 900 rpm to 1500 rpm at 1s and 5s with full load torque = 1.2 N.m.

## VI. CONCLUSION

This paper has presented a cost-effective vector control strategy for four switch three phase (FSTP) inverter fed a synchronous reluctance motor with conventional rotor (SynRM) drive. The major benefits of the proposed system are summarized below:

- A vector control strategy for FSTP inverter fed SynRM drive has been employed.
- The proposed system has various advantages compared to the conventional three phase six switch inverter namely, reduced number of power switches from six to four, improved the cost, reduced volume and high reliability.
- Mathematical and theoretical have presented along with selected simulation to support the proposed system.
- The control strategy is discussed for the proposed system with keeping the operation at maximum torque control.
- Both saturation and iron losses effects are considered to increase system accuracy.

Simulations and experimental results confirm the effectiveness of the proposed technique.

## REFERENCES

[1] J. K. Kostko, "Polyphase reaction synchronous motors," *J. Amer. Inst. Elec. Ing.*, Vol. 42, pp. 1162–1168, Nov. 1923.

[2] Feiqiu Tang ; Yaonan Tong ; Chunlai Li, "A controller for chaotic Synchronous Reluctance Motor drives system," *The Second IEEE International Conference on Computing, Control and Industrial Engineering (CCIE)*, 2011, vol. 2, pp. 316-319.

[3] Neti, P. ; Nandi, S., "Performance analysis of a reluctance synchronous motor under abnormal operating conditions," *Canadian Journal of Electrical and Computer Engineering*, vol. 33, Issue: 2, pp. 55-61, 2008.

[4] Chen, L. ; Wang, J. ; Lombard, P. ; Lazari, P. ; Leconte, V., "Design optimisation of permanent magnet assisted synchronous reluctance machines for electric vehicle applications," *XX$^{th}$ International Conference on Electrical Machines (ICEM)*, 2012, pp. 2647-2653.

[5] I. Boldea, L. Tutelea, and C. I. Pitic, "PM-assisted reluctance synchronous motor/generator (PM-RSM) for mild hybrid vehicles: Electromagnetic design," *IEEE Trans. on Ind. Appl.*, Vol. 40, No. 2, pp. 492–498, Mar./Apr. 2004.

[6] S. Saravanasundaram and K. Thanushkodi, "Compound Active Clamping Boost Converter-Three Phase Four Switch Inverter Fed Induction Motor," *International Journal of Computer Science and Network Security*, Vol. 8, No. 8, pp. 358-361, August 2008.

[7] M. N. Uddin, T. S. Radwan, and M. A. Rahman, "Performance Analysis of a Cost Effective 4-Switch, 3-Phase Inverter Fed IM Drive," *Iranian Journal of Electrical and Computer Engineering*, Vol. 5, No. 2, pp. 97-102, Summer-Fall 2006.

[8] M. N. Uddin, T. S. Radwan, and M. A. Rahman, "Fuzzy-Logic-Controller-Based Cost Effective Four-Switch ThreePhase Inverter-Fed IPM Synchronous Motor Drive System," *IEEE Trans. on Ind. Appl.*, Vol. 42, No. 1, pp. 21-30, Jan. /Feb. 2006.

[9] Phan Quoc Dzung, Le Minh Phuong, Tran Cong Binh, and Nguyen Minh Hoang, "A Complete Implementation of Vector Control for a Four-Switch Three-Phase Inverter Fed IM Drive," *International Symposium on Electrical & Electronics Engineering*, pp: 297 – 301, 24-25 Oct. 2007, HCM City, Vietnam.

[10] Longya Xu, Xingyi Xu, , Thomas A. Lipo, and Donald W. Novotny, "Vector Control of a Synchronous Reluctance Motor Including Saturation and Iron Loss, " *IEEE Trans. on Ind. Appl.*, Vol. 21, No. 5, pp: 977-985 Sep./Oct. 1991.

[11] Mostafa. A. Fellani and Dawo. E. Abaid, "Sliding-Mode Control of Synchronous Reluctance Motor," *International Journal of Electronics, Circuits and Systems*, Vol. 3, No. 2, pp. 91-95, 2009.

[12] Yamamoto, S. ; Ara, T. ; Matsuse, K., "A Method to Calculate Transient Characteristics of Synchronous Reluctance Motors Considering Iron Loss and Cross-Magnetic Saturation," *IEEE Transactions on Industry Applications*, vol. 43 , Issue: 1, pp. 47 – 56, 2007.

[13] Rashad, E.M. ; Radwan, T.S. ; Rahman, M.A., "A maximum torque per ampere vector control strategy for synchronous reluctance motors considering saturation and iron losses," *39$^{th}$ IAS Annual Meeting, IEEE Industry Applications Conference*, 2004, vol. 4, pp. 2411-2417